PROCEEDINGS OF SPIE

SPIEDigitalLibrary.org/conference-proceedings-of-spie

Alternative sampling functions for single-pixel imaging with a digital micromirror device

Susana Burnes-Rudecino, Lluís Martínez-León, Pere Clemente, Enrique Tajahuerce, Ma. Araiza-Esquivel

Susana Burnes-Rudecino, Lluís Martínez-León, Pere Clemente, Enrique Tajahuerce, Ma. Araiza-Esquivel, "Alternative sampling functions for single-pixel imaging with a digital micromirror device," Proc. SPIE 10932, Emerging Digital Micromirror Device Based Systems and Applications XI, 109320D (4 March 2019); doi: 10.1117/12.2508600

SPIE.

Event: SPIE OPTO, 2019, San Francisco, California, United States

Alternative sampling functions for single-pixel imaging with a digital micromirror device

Susana Burnes-Rudecino[a], Lluís Martínez-León[b], Pere Clemente[b,c], Enrique Tajahuerce[b], and Ma. Araiza-Esquivel[a]

[a]Unidad Académica de Ingeniería Eléctrica, Universidad Autónoma de Zacatecas (UAZ), Zacatecas 98000, México
[b]GROC-UJI, Institute of New Imaging Technologies (INIT), Universitat Jaume I, Castelló de la Plana 12071, Spain
[c]Servei Central d'Instrumentació Científica (SCIC), Universitat Jaume I, Castelló de la Plana 12071, Spain

ABSTRACT

Single-pixel imaging employs structured illumination to record images with very simple light detectors. It can be an alternative to conventional imaging in certain applications such as imaging with radiation in exotic spectral regions, multidimensional imaging, imaging with low light levels, 3D imaging or imaging through scattering media. In most cases, the measurement process is just a basis transformation which depends on the functions used to codify the light patterns. Sampling the object with a different basis of functions allows us to transform the object directly onto a different space. The more common functions used in single-pixel imaging belong to the Hadamard basis or the Fourier basis, although random patterns are also frequently used, particularly in ghost imaging techniques. In this work we compare the performance of different alternative sampling functions for single pixel imaging, all of them codified with a digital micromirror device (DMD). In particular, we analyze the performance of the system with Hadamard, cosine, Fourier and noiselet patterns. Some of these functions are binary, some others real and other complex functions. However, all of them are codified with the same DMD by using different approaches. We perform both numerical and experimental tests with the different sampling functions and we compare the performance in terms of the efficiency and the signal-to-noise ratio (SNR) of the final images.

Keywords: Computational imaging, single-pixel imaging, spatial light modulator, structured light

1. INTRODUCTION

Among the different technologies of spatial light modulators, DMDs, which were invented at Texas Instruments in 1987,[1] are the most considered in applications requiring a quick response. A DMD is formed by thousands of micromirrors that modulate the input light according to just two possible states: the on state reflects the light into the desired optical path and the off state rejects it. Because their high speed and simple control, DMDs have been used for engineering light in different areas of research, such as wavefront formation[2] and single-pixel imaging (SPI).[3] SPI techniques, which are closely related to ghost imaging,[4] have revealed themselves as an alternative imaging approach in a broad range of topics: holography,[5] hyperspectral imaging,[6] seeing through scattering media,[7,8] 3D imaging[9] and microscopy.[10] In all these cases, a device without spatial resolution is used for detection, which is certainly convenient when employing radiation in exotic spectral regions out of the visible spectrum or imaging with low light levels. Besides, the approach is very well adapted to multidimensional sensing. In a SPI system, the object is sampled by using structured light. Thus, sampling light patterns are projected onto the object and the resulting total irradiances are registered with a bucket detector. The image of the object is reconstructed by means of computational algorithms. The resolution of the image is related to that of the sampling patterns. The measurement process in SPI can be considered as a basis transformation were the

Further author information: (Send correspondence to S.B.R.)
S.B.R.: E-mail: sl_burnesr@uap.uaz.edu.mx, Telephone: +52 (492) 136 01 34

Emerging Digital Micromirror Device Based Systems and Applications XI, edited by Michael R. Douglass, John Ehmke, Benjamin L. Lee, Proc. of SPIE Vol. 10932, 109320D
 · doi: 10.1117/12.2508600

functions of the new basis are the sampling light patterns. In this communication, we analyze the performance of different sampling patterns codified with a DMD and describe their operation in detail. As a DMD is a binary amplitude device, different strategies are required to implement real and complex functions onto the DMD. Hadamard, cosine, noiselet and Fourier functions have been studied with simulations and experiments. The SNR has been used to validate the quality of the reconstructed images. The remaining of this communication is structured as follows. Section 2 presents these four different bases and explains how they can be used with a DMD in an SPI system. The optical setup used in this work is described in Section 3, and the experimental results are shown in Section 4. Finally, conclusions are summarized in Section 5.

2. BASIS CODIFICATION

The selection of the basis of functions used to image an object in SPI depends on a number of factors, including the characteristics of the object, the compression efficiency, or the available methods for pattern codification. Each transformation provides different results.

The Hadamard transform has real coefficients and involves just algebraic operations. It is used to encode, detect or compress images. It redistributes the energy of the image over the low frequencies. Its codification is straightforward and its experimental implementation is fast.[11] The Walsh-Hadamard functions are codified with sampling light patterns. The only two possible values are $+1$ and -1. An example of a 3×3 basis is shown in Figure 1(a). Therefore, two matrices are necessary to codify the corresponding transform functions in a DMD. The first matrix contains the positive values, where the $+1$ values are kept and the negative values are changed to 0ś. The second matrix is projected with the negative values as $+1$ and the positive values turned to 0ś. The Walsh-Hadamard coefficients are then obtained as the difference of the coefficients provided by matrices H_+ and H_-. Therefore, the number of required measurements is doubled: an image of 64×64 pixels needs 2×4096 Hadamard patterns to be displayed. In order to reduce measurement and processing time, optimization algorithms, like compressed sensing in the case of sparse signals, can be employed. These kind of compressive strategies can be employed also with the following transformations discussed in the paper.[12]

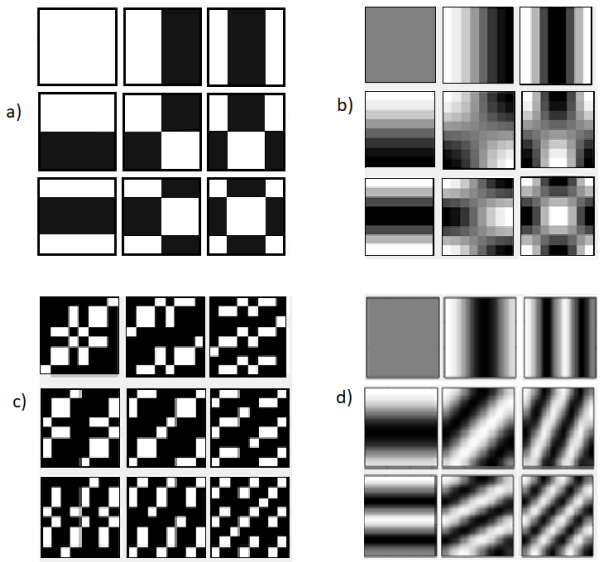

Figure 1. Representation of different basis: a) Hadamard, b) cosine, c) noiselet and d) Fourier.

Functions of the cosine basis have real values, within the range of -1 to $+1$. This basis transform also concentrates the signal energy in the low frequencies, making it appropriate for applications where data compression is a must.[13] Figure 1(b) shows an example of sampling functions of a 3×3 cosine basis. Cosine patterns need to be adapted to be codified in a DMD. In the human vision process, the eye can perceive gray shades

from binary dithered images at a certain distance. Likewise, conversion of cosine functions into binary functions is the key to codify these patterns on a DMD. The cosine function has to be scaled to a k factor and then binarized by dithering. This recreates the impression of gray levels in a white and black image just consisting of 1 and 0 values. In our experiments, the best performance is achieved by dithering with the Floyd-Steinberg error diffusion algorithm.[14] Figure 2 shows dithering in the cosine pattern of frequency $(1, 2)$. To obtain the corresponding transform coefficient, two patterns, C_+ and C_-, are projected, in order to calculate the difference of their corresponding coefficients. The number of measurements is doubled again.[15] Thus, 2×4096 cosine patterns are used for an image of 64×64 pixels.

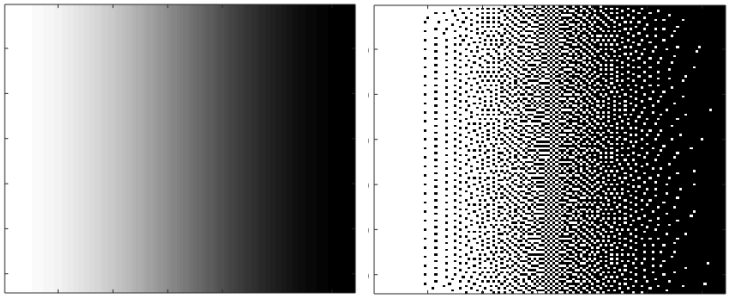

Figure 2. a) Real basis cosine and b) cosine basis with dithering effect.

The two transformations analyzed above correspond to real functions. However, there are also other examples with complex values, like the noiselet transform. It presents four possible values, $+1$, -1, $+i$ and $-i$, but the implementation onto a DMD is also straightforward. After its binary adaptation, the signal energy is spread over all the frequency range. Due to its high incoherence with the wavelet transform, it is commonly used in compressed sensing.[16] In Figure 1(c) the real part of a noiselet pattern is shown. To codify this transform with a DMD, each noiselet pattern is separated in four matrices. Similarly to the Hadamard basis implementation, two matrices contain integer values where the imaginary values are set to zero. Then, two more matrices are set to $+1$ for the imaginary values and zero for the integer values. Thus, the corresponding difference equation is the combination of four matrices, R_{N_+}, R_{N_-}, I_{N_+} and I_{N_-}.[17] And these four matrices have to be projected on the DMD to obtain the corresponding complex transform coefficient. Processing time is increased as the number of matrices displayed onto the DMD is higher: 4×4096 patterns are needed to transform an image of 64×64 pixels. The Fourier transform is one of the most important tools in signal processing, and subsequently in image processing.[13] This transform provides information in the frequency domain. It has been applied to encode or retrieve data with high quality. Nevertheless, the time for transforming and recovering the information is long.[18] Indeed, Fourier transform is also a complex function requiring changes to be programmed onto the DMD. The complex basis is modified using phase shifting, one of the most robust and common methods of creating real Fourier patterns.[19] In this case, a group of sinusoidal functions with a phase shift of $\pi/4$ is generated. Moreover, it is necessary to convert these patterns into binary functions, by scaling them k times and applying dithering, as explained previously for the cosine transform. Figure 1(d) shows the real part of a 3×3 Fourier basis. Four patterns are displayed on the DMD for each Fourier coefficient, F_0, $F_{\pi/4}$, $F_{\pi/2}$ and $F_{3\pi/4}$. After measurements are made, the recorded total irradiances are combined to get the corresponding complex coefficient.[17] If the image has 64×64 pixels, the number of measurement is 4×4096. As the coefficients are obtained in the Fourier space, reconstruction of the object image requires an inverse Fourier transform operation.

3. EXPERIMENTAL SETUP

The experimental setup of the SPI system used in this work is shown in Figure 3. The light source is a fiber-coupled solid-state laser with a wavelength of 532 nm (Oxxius-532-50-COL-SLM). A lens L_c colimates the light beam and illuminates the DMD. The spatial light modulator is a DLP Discovery 4200 by Texas Instruments with a pixel pitch of 13.7 μm. This DMD has a resolution of 1024×768 micromirrors, which can be tilted individually via the controlling interface software. In the on state, mirrors are tilted about the diagonal hinge at an angle

of $+12°$, and at $-12°$ in the off state. For this study Hadamard, cosine, noiselet and Fourier basis have been programmed onto the DMD with a spatial resolution of 64×64 pixels. A pixel in each basis studied corresponds to 8×8 micromirrors. Then, the active area of the DMD is $7.06 \times 7.06\ mm^2$. The structured light provided in reflection by the DMD travels through the $4f$ optical imaging system, formed by lenses L_1 and L_2, both with focal distance $f = 250$ mm. At the image plane, the inner product of the object and each projected pattern produces different irradiances, collected by lens L_3 in a Thorlabs $PDA36A$ photo-detector. The photocurrent signals are digitized by a data acquisition device, and then the calculated coefficients are computed to reconstruct the object image.

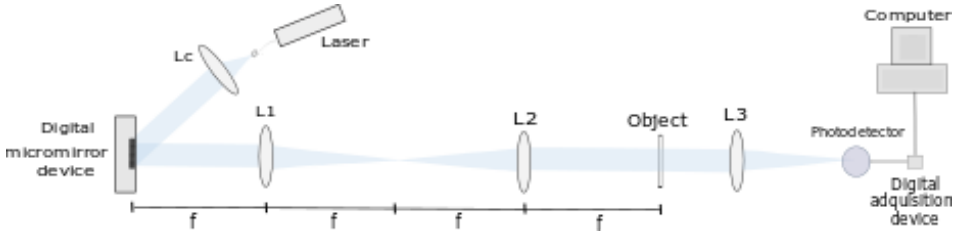

Figure 3. Experimental setup of the SPC.

4. RESULTS

The experimental results are shown in Figure 4. A transparency with the logo of Universitat Jaume I has been used as object. The images obtained have a resolution of 64×64 pixels. Differences between the reconstructions are noticeable, depending on the transform basis used. The particular response for each basis is also evident in the corresponding spectral representations (not shown here). To quantify the image quality of each of the reconstructions, the SNR has been calculated according to the expression $SNR = \frac{\sigma^2_{signal}}{\sigma^2_{noise}}$. The retrieved image from the Hadamard sampling patterns is illustrated in Figure 4(a). This image presents high contrast and an SNR of 50.78 dB. The reconstruction when measuring with the cosine basis is shown in Figure 4(b). This image presents undesired terms possibly due to the process to transform continuous cosine patterns to binary functions. Even with the chess-table effect present on the retrieved image, the SNR is 42.28 dB. As seen in Figure 4(c), the image obtained with the noiselet transform presents an artifact affecting the whole image. High frequency components are emphasized by this transform, reducing the quality of the reconstruction. The SNR here is 23.6 dB. Finally, for the case of the Fourier patterns, shown in Figure 4(d), reconstruction is satisfactory, even if the patterns were transformed from continuous to binary values. SNR in this case is 78.60 dB. Simulations had also been carried out, providing quality reconstructions with all the bases. For the noiselet, simulation provides a reconstruction without the problems of the experimental image.

5. CONCLUSIONS

This communication presents a study of the performance of the most common basis functions used in SPI (Hadamard, cosine, noiselet and Fourier), because of their versatility in compression and codification and easy implementation. The procedure to display these real and complex bases in a binary amplitude device as a DMD has been explained in detail. Experimental reconstructions using each of these bases are presented. Hadamard and Fourier sampling functions provide high quality images, although modifications have been applied in the modulation patterns to be able to implement them in a DMD. For cosine and noiselet patterns, some undesirable frequencies are present. The increase in the measurement and processing time caused by the implementation of real and complex values in a binary amplitude modulator could be overcome by using algorithms of optimization as compressed sensing.

ACKNOWLEDGMENTS

This work has been supported by CONACYT and Universidad Autónoma de Zacatecas. S. Burnes acknowledges them for partial financial support.

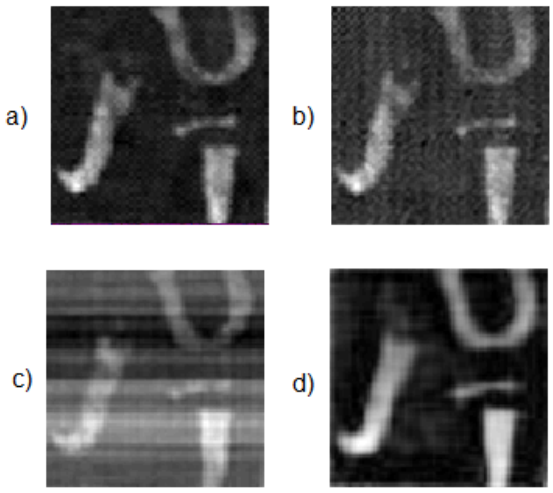

Figure 4. Recovered images from SPI using a) Hadamard patterns, b) cosine patterns, c) noiselet patterns and d) Fourier patterns.

REFERENCES

[1] Hornbeck, L. J., "Digital light processing and mems: Timely convergence for a bright future (invited paper)," in [*Micromachining and Microfabrication Process Technology*], *Proc. SPIE* **2639**, 2–20 (1995).

[2] Ren, Y., Lu, R., and Gong, L., "Tailoring light with a digital micromirror device," *Ann. Phys.* **527**(7-8), 447–470 (2015).

[3] Wakin, M. B., Laska, J. N., Duarte, M. F., Baron, D., Sarvotham, S., Takhar, D., Kelly, K. F., and Baraniuk, R. G., "An architecture for compressive imaging," in [*Proceedings of the International Conference on Image Processing (ICIP 2006)*], 1273–1276 (2006).

[4] Khamoushi, S. M. M., Nosrati, Y., and Tavassoli, S. H., "Sinusoidal ghost imaging," *Opt. Lett.* **40**, 3452–3455 (Aug 2015).

[5] Clemente, P., Durán, V., Tajahuerce, E., Andrés, P., Climent, V., and Lancis, J., "Compressive holography with a single-pixel detector," *Opt. Lett.* **38**(14), 2524–2527 (2013).

[6] Rueda-Chacón, H. F., Vargas-García, C. A., and Arguello-Fuentes, H., "Single-pixel optical sensing architecture for compressive hyperspectral imaging," *Revista Facultad de Ingeniería Universidad de Antioquia* (73), 124–133 (2014).

[7] Rodríguez, A., Clemente, P., Irles, E., Tajahuerce, E., and Lancis, J., "Resolution analysis in computational imaging with patterned illumination and bucket detection," *Opt. Lett.* **39**(13), 3888–3891 (2014).

[8] Xu, Y.-K., Liu, W.-T., Zhang, E.-F., Li, Q., Dai, H.-Y., and Chen, P.-X., "Is ghost imaging intrinsically more powerful against scattering?," *Opt. Express* **23**(26), 32993–33000 (2015).

[9] Yu, W.-K., Yao, X.-R., Liu, X.-F., Li, L.-Z., and Zhai, G.-J., "Three-dimensional single-pixel compressive reflectivity imaging based on complementary modulation," *Appl. Optics* **54**(3), 363–367 (2015).

[10] Rodriguez, A., Clemente, P., Tajahuerce, E., and Lancis, J., "Dual-mode optical microscope based on single-pixel imaging," *Opt. Lasers Eng.* **82**, 87–94 (2016).

[11] Pratt, W., Kane, J., and Andrews, H., "Hadamard transform image coding," *Proceedings of the IEEE* **57**(1), 58–68 (1969).

[12] Duarte, M., Davenport, M., Takhar, D., Laska, J., Sun, T., Kelly, K., and Baraniuk, R., "Single-pixel imaging via compressive sampling," *IEEE Signal Process. Mag.* **25(2)**, 83–91 (2008).

[13] Gonzalez, R. and P., W., [*Digital Image Processing*], Addison-Wesley, New Jersey (2002).

[14] Zhang, Y., [*Image processing*], vol. 1, Walter de Gruyter GmbH & Co KG (2017).

[15] Liu, B.-L., Yang, Z.-H., Liu, X., and Wu, L.-A., "Coloured computational imaging with single-pixel detectors based on a 2d discrete cosine transform," *J. Mod. Optic* **64**(3), 259–264 (2017).

[16] Candès, E., Romberg, J., and Tao, T., "Robust uncertainty principles: Exact signal reconstruction from highly incomplete frequency information," *IEEE Trans. Inform Theory* **52**(2), 489–509 (2006).

[17] Zhang, Z., Ma, X., and Zhong, J., "Single-pixel imaging by means of fourier spectrum acquisition," *Nat. Comm.* **6**, 6225 (2015).

[18] Zhang, Z., Wang, X., Zheng, G., and Zhong, J., "Fast fourier single-pixel imaging via binary illumination," *Sci. Rep.* **7**(1), 12029 (2017).

[19] Zhang, Z., Wang, X., Zheng, G., and Zhong, J., "Hadamard single-pixel imaging versus fourier single-pixel imaging," *Opt. Express* **25**(16), 19619–19639 (2017).